1.55-μm Si-based MOEMS optical tunable filter

Yuhua Zuo (左玉华), Changjun Huang (黄昌俊), Buwen Cheng (成步文), Xiao Cai (蔡 晓), Rongwei Mao (毛容伟), Chuanbo Li (李传波), Liping Luo (罗丽萍), Junhua Gao (高俊华), Yunxia Bai (白云霞), Lei Jiang (姜 磊), Chaohua Ma (马朝华), Jialian Zhu (朱家廉), Liangchen Wang (王良臣), Jinzhong Yu (余金中), and Qiming Wang (王启明)

State Key Joint Laboratory on Integrated Optoelectronics, Institute of Semiconductors, Chinese Academy of Sciences, Beijing 100083

Received March 25, 2003

A prototype 1.55-μm Si-based micro-opto-electro-mechanical-systems (MOEMS) tunable filter is fabricated, employing surface micromachining technology. Full-width-at-half-maximum (FWHM) of the transmission spectrum is 23 nm. The tuning range is 30 nm under 50-V applied voltage. The device can be readily integrated with resonant cavity enhanced (RCE) detector and vertical cavity surface emitting laser (VCSEL) to fabricate tunable active devices.

OCIS codes: 350.2460, 220.4000, 130.3120.

Tunable optical filter plays an important role in the tremendously developed dense-wavelength-division-multiplexing (DWDM) system. It also finds applications in beam steering and spectrum analyzing. A wide continuous wavelength tuning range is desirable in these applications. However, the tuning range of traditional tunable technologies, such as thermo-optical tuning[1], has been limited to about 10 nm. Micro-opto-electro-mechanical-systems (MOEMS) tunable technology gains great attention worldwide for its advantage to obtain large tuning range and potential low cost[2−5]. Compared with the traditional Bragg grating filters and multiple film filters, MOEMS tunable filter can integrate wide tuning range with compactness and compatibility with mature IC technology. The famous groups are J. S. Harris group of Stanford[3], C. Chang group of U. C. Berkeley[4], and Y. H. Lo group[5] of Cornell University (now in U. C. San Diego). The former two groups focus on 980-nm tunable vertical cavity surface emitting laser (VCSEL), and the latter has demonstrated long wavelength wafer bonding GaAs-based tunable photodetector/LED.

In this letter, we report a 1.55-μm Si-based MOEMS tunable optical filter, using our own patent surface micromachining technology. Such filter is based on a Fabry-Perot (F-P) interferometer, consisting of two parallel mirrors with high reflectivity. The bandwidth of its transmittance spectrum is characterized by full-width-at-half-maximum (FWHM)[5]:

$$\mathrm{FWHM} = \frac{\lambda_0^2(1-\sqrt{R_1R_2})}{2\pi n L_0 (R_1R_2)^{\frac{1}{4}}}, \tag{1}$$

where R_1 and R_2 denote the reflectivity of the top and bottom mirrors, λ_0 is the center wavelength, L_0 is the initial cavity length, and n is the refractive index of the cavity. The transmittance wavelength of F-P cavity depends on the cavity length, and the wavelength shift changes linearly with the cavity length change

$$\frac{\Delta\lambda}{\lambda_0} = \gamma\frac{\Delta L}{L_0}, \tag{2}$$

where $\Delta\lambda$ is the wavelength shift, ΔL is the cavity length change, and γ is a constant dependent on the optical structure of the filter.

During wavelength tuning, a dc voltage is applied between the top and bottom electrode, creating an electrostatic force that attracts the suspended membrane toward the substrate surface. Therefore, the effective F-P cavity length is shortened with the applied voltage, resulting in a blue shift of its center wavelength. The relation between the electrostatic force F and the applied voltage U is given by

$$F = \frac{\varepsilon A}{2L_0^2}U^2, \tag{3}$$

where A denotes the effective area of the electrode, and ε is permittivity of air. As the cavity length change is proportional to the electrostatic force, combining the Eqs. (2) and (3), it can be derived that the wavelength shift is quadratic to the applied voltage.

The device is shown schematically in Fig. 1. Starting material was an n-type ⟨100⟩ double polished silicon substrate. After boron implantation and rapid thermal annealing, p^{++} layer was formed as the bottom electrode. 3.5 pairs of quarter wavelength Si/SiO_2 were grown by electron beam evaporation to form bottom distributed Bragg reflector (DBR). A sacrificial layer was used to form an air gap between the suspended structure and the bottom electrode. Its thickness was controlled to

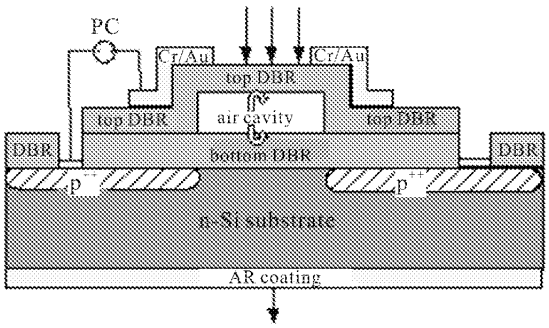

Fig. 1. Schematic structure of the cross-section of the tunable MOEMS filter.

be about half of the center wavelength 1550 nm. The top DBR of 3 pairs of Si/SiO_2 was deposited on the sacrificial layer, followed by Cr/Au top electrode. A 220-nm-thick silicon nitride layer was then deposited by plasma-enhanced chemical vapor deposition (PECVD) on the bottom of the substrate as anti-reflection (AR) coating. After dry etching of patterned DBR, contact holes were made through the DBR layers to have electric access to the bottom electrode. The final suspended structure was released after the removal of the sacrificial layer.

The diamond membrane, with the size of 150 × 150 μm^2, is supported by four cantilever beams. The optical window is a 150 × 150 μm^2 square. The beams of different devices are 20 – 50 μm wide and 100 – 150 μm long. The supporting beams are made up of top DBR and top electrode Cr/Au, with the total thickness of around 5 μm. A scanning electron microscopy (SEM) micrograph is shown in Fig. 2.

The transmission characteristics of the devices were measured using two multimode fibers for input and output light coupling. A tungsten lamp light covering a spectral range of 0.8 – 1.8 μm was used to provide the input light. The light that passed through the tunable filter was coupled into the output fiber and detected by an optical measuring system.

Figure 3 shows the transmittance spectra of the tunable filter under applied voltage from 0 to 50 V. The center wavelength is continuously tuned from 1698.3 nm at 0 V to 1668.3 nm at 50 V. The intensity of the peak

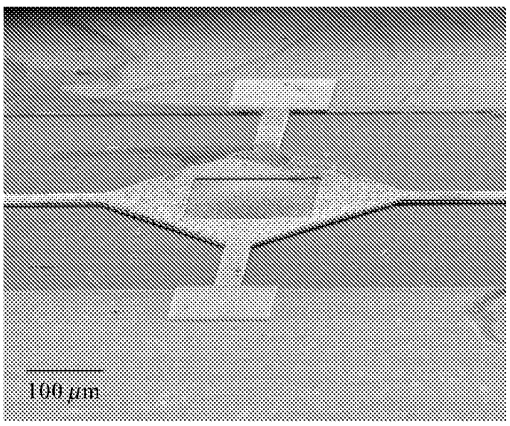

Fig. 2. SEM micrograph of the device structure.

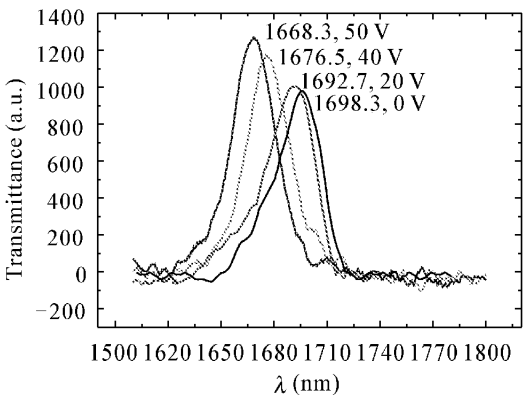

Fig. 3. Transmittance spectra of the tunable filter versus applied voltage.

increases slightly when the wavelength decreases. We attribute it to the response dependence on wavelength of the InGaAs detector, whose response decreases with the increasing wavelength in the range of 1500 – 1750 nm. The largest peak intensity change is 30% at 1668.3 nm, compared with the initial peak intensity at 1698.3 nm.

The FWHM of the transmittance spectrum at 0 V is about 23 nm. However, using the designed values of L_0 850 nm, R_1 and R_2 99% and 99%, and the center wavelength λ_0 1700 nm, the calculated FWHM from Eq. (1) is 5.4 nm. The large discrepancy between them is mainly due to the mirror reflectivities lower than designed. When R_1 and R_2 are 93.5% and 98%, the calculated FWHM is 23.4 nm. It is evident that the FWHM of a F-P cavity with short cavity length is strongly influenced by the mirror reflectivities. In addition, the undulation of the sacrificial layer also contributes to the decrease of top mirror reflectivity. If the quality of the sacrificial layer is improved and the reflectivities of top and bottom mirror increase to 99.5%, the FWHM can be reduced to 2.7 nm. Further work is under way to reduce the obvious wide FWHM.

The spectra at 0 V and 20 V are asymmetric, having a long tail on the short wavelength side. It is possible induced by the curvature of the released top mirror. Using nonlinear fit of Gaussian model, the transmittance spectrum at 0 V can be divided into two separate peaks P1 and P2, as shown in Fig. 4. The whole cavity can be modeled as two parallel F-P cavities with different cavity lengths. The length of the longer cavity (corresponding to P1) decreases quickly when the voltage increases. By contrast, the length of the shorter one (corresponding to P2) decreases slightly with the increasing voltage. It indicates that the longer cavity locates near the center of the mirror, where the vertical displacement is larger, while the shorter cavity with the smaller vertical displacement locates in the edge of the mirror. The initial top mirror is convex, as shown in Fig. 2. As the voltage increases further, the vertical displacement of the center part of the mirror is larger than the edge; the mirror becomes flatter, P1 moves near P2. Thus the symmetry of transmittance spectrum at higher voltage (40 V) improves. Local heat treatment of the mirror or using smaller mirror may relieve the stress-induced mirror curvature.

The wavelength shifts dependence on applied voltage

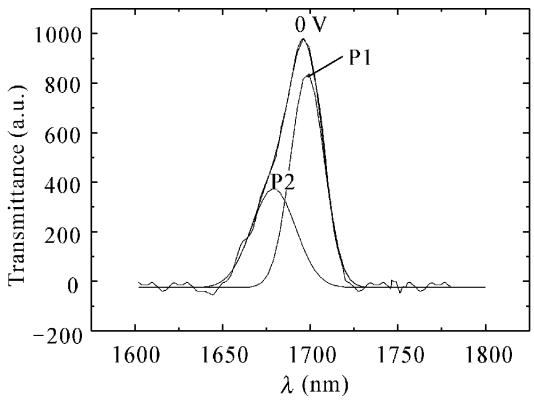

Fig. 4. Analysis of transmittance spectra of the tunable filter at zero voltage.

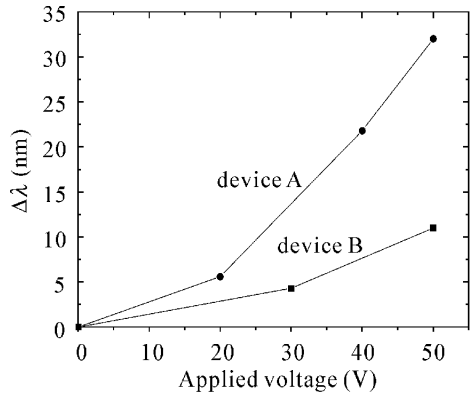

Fig. 5. Wavelength shift as a function of tuning voltage for devices with different beam stiffness.

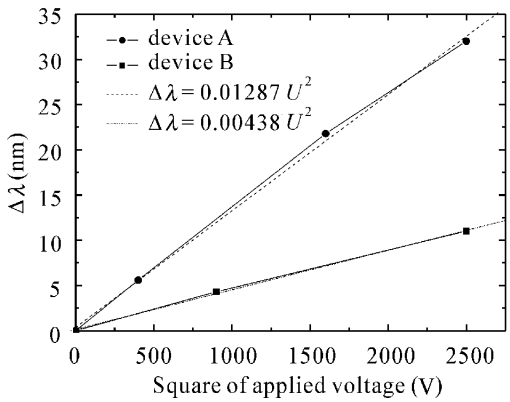

Fig. 6. Wavelength shift dependence on square of applied voltage for devices with different beam stiffness.

for two devices with different beam stiffness, described as device A and device B, are shown in Fig. 5. The beam of device A is 150 μm long, and 30 μm wide, while the beam of device B is 100 μm long, and 20 μm wide. Their corresponding wavelength shifts are 30 and 10 nm, respectively. The wavelength shifts as a function of square of applied voltage is shown in Fig. 6. It is obvious that they have good linear relationship. The tuning coefficients of device A and device B are calculated to be 0.01287 and 0.00438 nm/V^2, respectively. In other words, the wavelength will shift 1.2 and 0.4 nm, respectively, under 10 V. Since the top and bottom dielectric DBRs (consisting of 8.5 pairs of Si and SiO_2) lie between the two electrodes, they will reduce the effective voltage applying on the air gap. And the electrode configuration also affects the electric field distribution. It is estimated that only 30% applied voltage has contribution to tuning. The tuning voltage can be further reduced by optimizing the electrical field, as well as improving the mechanical structure of the beams.

In conclusion, we have demonstrated a Si-based 1.55-μm MOEMS tunable optical filter with a continuous tuning range of 30 nm, by surface micromachining technology. The technology is substrate independent and has wide applications in DWDM system. It can be easily integrated with vertical cavity devices, such as RCE detector and VCSEL, to achieve active tunable devices.

The project was supported by the Major State Basic Research (973) Program of China (No. G2000036603), the National Natural Science Foundation of China (No. 96104003) and 863 Plan of China (No. 2002AA312010). Y. Zuo's e-mail address is yhzuo@red.semi.ac.cn.

References

1. D. Hohlfeld, M. Epmeier, and M. Zappe, Sensors and Actuators A **93,** 103 (2003).
2. P. Tayebati, P. Wang, and M. Azimi, Electron. Lett. **34,** 1967 (1998).
3. F. Sugihwo, M. C. Larson, and J. S. Harris, J. Micro-Electro-Mechanical Systems **7,** 48 (1998).
4. C. J. Chang-Hasnain, IEEE J. Selected Topics in Quantum Electron. **6,** 978 (2000).
5. A. T. T. D. Tran, Y. H. Lo, Z. H. Zhu, D. Haronian, and E. Mozdy, IEEE Photon. Technol. Lett. **8,** 393 (1996).